GlueX-doc-1432
SVN: docs/GlueXdoc/sipm_guides
Original: February 18, 2010
Update: February 26, 2010

# Trapezoidal guides for the light collection for SiPMs

E.S. Smith

## 1 Introduction

The project has selected SiPMs to be used for the light sensors for the Barrel Calorimeter (BCAL) readout. Having decided on the sensor that is to be used, we now have the task of detailing the light collection, the final configuration for the electronics, the mechanical attachments, scheme for temperature stabilization, all input and output connections to the light-tight enclosure, and proceed with many other configuration choices. In this study, we calculate the expected light collection from the end of the BCAL module to the light sensors using acrylic light guides. Of particular interest is the impact of different possible optical contacts between the light guides and the sensors, which can have important implications for the mechanical attachment and assembly of sensors, light guides and electronics.

## 2 Setup and Geometry

The light collection has been simulated using GEANT3 [1] in a procedure described in more detail in previous notes [2, 3, 4]. The trajectories of light rays through the light guide were propagated using the standard PHYS260 package for "Cerenkov Photons." The photons that are relevant to this study are in the visible spectrum but the optical properties from the "Cerenkov" package cover this part of the spectrum as well. The parameters of the materials are the same as those described previously, if not specified here.

Fig. 1 is a sketch of the face of the BCAL covered with a layout of the proposed shapes for the base of the light guides for the SiPMs. This arrangement was devised to minimize the number of different light guide shapes and to keep the projected angles of the shapes to 90° and 86.25°. This configuration results in a total of 20 different shapes for the 40 SiPMs. The shapes of the light guides are illustrated in Fig. 2. The length of the guides is 8 cm, and the effects of air gaps were studied by inserting a (thin) rectangular volume at the entrance (referred to as Gap2) and exit

(Gap1) of the light guide. The material in the gap is set to either air or lucite (light guide material) for ease of switching between configurations. At the exit, Gap1 was followed by a 1 mm window, and 1 mm sensitive volume. The window, taken to be lucite in the present simulation, represents the cover over the SiPM [1]. The output area is a $1.2\times1.2$ cm$^2$ square, which represents the sensitive area of the SiPMs.

The collection efficiencies were calculated for an input distribution of light rays which was uniform over the entrance area and uniform in $\cos\theta$ up to the maximum trapping angle $\theta_{max}$ in the fiber (see Fig. 3). For direct coupling of light guides to the BCAL and air at the exit Gap1, we take $\theta_{max}$ to be 26.7°. For the case of an entrance air gap (Gap2), we take $\theta_{max}$ to be 45.7°. An optical ray reaching the sensitive SiPM volume was reported as the successful detection of a photon. A summary of the collection efficiencies for the nominal light guide length of 8 cm and gap width of 1 mm are given in Table 1. The collection efficiencies are tabulated in Table 2 as a function of light guide length for the nominal 1 mm Gap1 width at the entrance. We see that the efficiencies are very weakly dependent on the length of the guide for lengths greater than 4 cm. Therefore, in the rest of the study has kept the light guide length at 8 cm.

# 3 Efficiencies

The light collection efficiency is plotted as a function of the transverse horizontal dimension $x$ in Figs. 4, 5 and 6. The efficiencies are rather uniform, although they increase slightly for the air Gap1 at the edge where the angle of the light guide is cut to conform to the face of the BCAL configuration. The efficiencies as a function of the vertical input dimension $y$ are shown in Figs. 7, 8 and 9. Here the air Gap2 configuration suffers from considerable loss of efficiency at the top and bottom of the light guide. The input and output azimuthal and polar angles are shown in Figs. 10, 11 and 12. The correlations between input and output polar angles are shown in Figs. 13, 14 and 15, which shows that the light rays with angles larger than 42° are not transmitted through the exit air Gap1. This significantly reduces the acceptance of light collection with an air gap between the light guide and sensor. The exit locations of light rays that fail to reach the sensitive volume are plotted in Figs. 16, 17 and 18. By comparing the bottom left figures of these two plots, one can see that when an air gap is present a significant fraction of photons bounce off the end of the light guide, returning to the entrance of the light guide and getting lost out the front. In addition, a significant number of photons exit in the region between the end of the light guide and the sensitive volume (in both the air gap and the window). These are light rays exiting at the outside edges of the light guide. For the air Gap2 between

[1] The window will be made of clear epoxy.

the BCAL and the guide, most of the light is lost at the entrance to the light guide at the perimeter, causing non-uniformities in the collection of light coming out of the BCAL.

The simulations show that the collected light is well-mixed as it passes through the light guide. We show that there is very little correlation between the input and exit locations of light rays in Figs. 19, 20 and 21. The collection efficiency is therefore relatively uniform over the input face of the BCAL when there is a gap at the exit. This is good because it reduces systematics arising from gain variations in the light sensors. In the case of the entrance air gap (Gap2), the losses in the perimeter are quite noticeable.

# 4 Summary and conclusions

A summary of the geometrical configurations studied and the efficiencies for the nominal gap width of 1 mm are given in Table 1. Of course, it is also of interest to understand the dependence of the light collection efficiency on the gap size. We computed the efficiency for the air and lucite gaps for different gap sizes, which are plotted in Fig. 22. The plot shows that there is a finite collection efficiency even at zero gap, where the efficiency for an air gap at the exit is about 2/3 that of a lucite gap, which is about 88%. The efficiency decreases linearly as the gap size increases, but the dependence is much sharper for an air gaps than it is for a lucite gap. For a gap of 1 mm, the efficiency of the exit air Gap1 has decreased to about 53% of the efficiency for the lucite gap, and for the entrance air Gap2 the collection efficiency is 69%. The collection efficiency when there is a gap at both the entrance and exit is approximately the product of the individual collection efficiencies, which shows that the losses are roughly independent. We note that the loss of efficiency for Gap2 around the outside edges of the light guide creates non-uniform position-dependent losses for light on the exit face of the BCAL. This non-uniformity can have serious impact on energy resolution. However, this light can be recovered in adjacent light guides at the expense of some "cross-talk" between segments.

# References

[1] Computing CERN Application Software Group and Networks Division. Geant detector description and simulation tool. http://wwwasd.web.cern.ch/wwwasd/geant, 1993.

[2] E.S. Smith. Light guide collection for the bcal outer layers. GlueX-doc-959, 2008.

[3] E.S. Smith. Light collection for light guides for use with fine mesh pmts for the bcal readout. GlueX-doc-1077, 2008.

[4] E.S. Smith. Reference calculations for light collection for light collection for fine mesh pmts. GlueX-doc-1287, 2009.

Table 1: Collection efficiency for various trapezoidal configurations for the nominal guide length of 8 cm. The attenuation length in the light guide was set to 240 cm. The ratio of output to input areas is 29% for the rectangle and 23% for the circular output. For reference a Winston Cone shape calculation is also given.

| Configuration | Top (cm) | Side (cm) | Bottom (cm) | Length (cm) | Output Square (cm) | Gap (mm) | Eff (%) |
|---|---|---|---|---|---|---|---|
| SiPM rect Inner outside top | 2.525 | 2.0 | 2.4026 | 8 | 1.2×1.2 | Lucite (2mm) | 87.1 |
| SiPM rect Inner outside top | 2.525 | 2.0 | 2.4026 | 8 | 1.2×1.2 | Air Gap 2 (1mm) | 69.1 |
| SiPM rect Inner outside top | 2.525 | 2.0 | 2.4026 | 8 | 1.2×1.2 | Air Gap1 (1mm) | 52.5 |
| SiPM WC inner outside top | 2.525 | 2.0 | 2.4026 | 2+6+2.13 | circle R=0.6 | None | 81.2 [3] |



Table 2: Collection efficiency as a function of the length of the guide for a 1mm exit Gap1. The collection efficiency is rather insensitive to the guide length for lengths greater than 4cm.

| Configuration | Top (cm) | Side (cm) | Bottom (cm) | Length (cm) | Output Square (cm) | Gap (mm) | Eff (%) |
|---|---|---|---|---|---|---|---|
| SiPM rect Inner outside top | 2.525 | 2.0 | 2.4026 | 2 | 1.2×1.2 | Air Gap1 (1mm) | 44.8 |
| SiPM rect Inner outside top | 2.525 | 2.0 | 2.4026 | 4 | 1.2×1.2 | Air Gap1 (1mm) | 52.7 |
| SiPM rect Inner outside top | 2.525 | 2.0 | 2.4026 | 8 | 1.2×1.2 | Air Gap1 (1mm) | 52.5 |
| SiPM rect Inner outside top | 2.525 | 2.0 | 2.4026 | 12 | 1.2×1.2 | Air Gap1 (1mm) | 52.0 |
| SiPM rect Inner outside top | 2.525 | 2.0 | 2.4026 | 16 | 1.2×1.2 | Air Gap1 (1mm) | 50.3 |

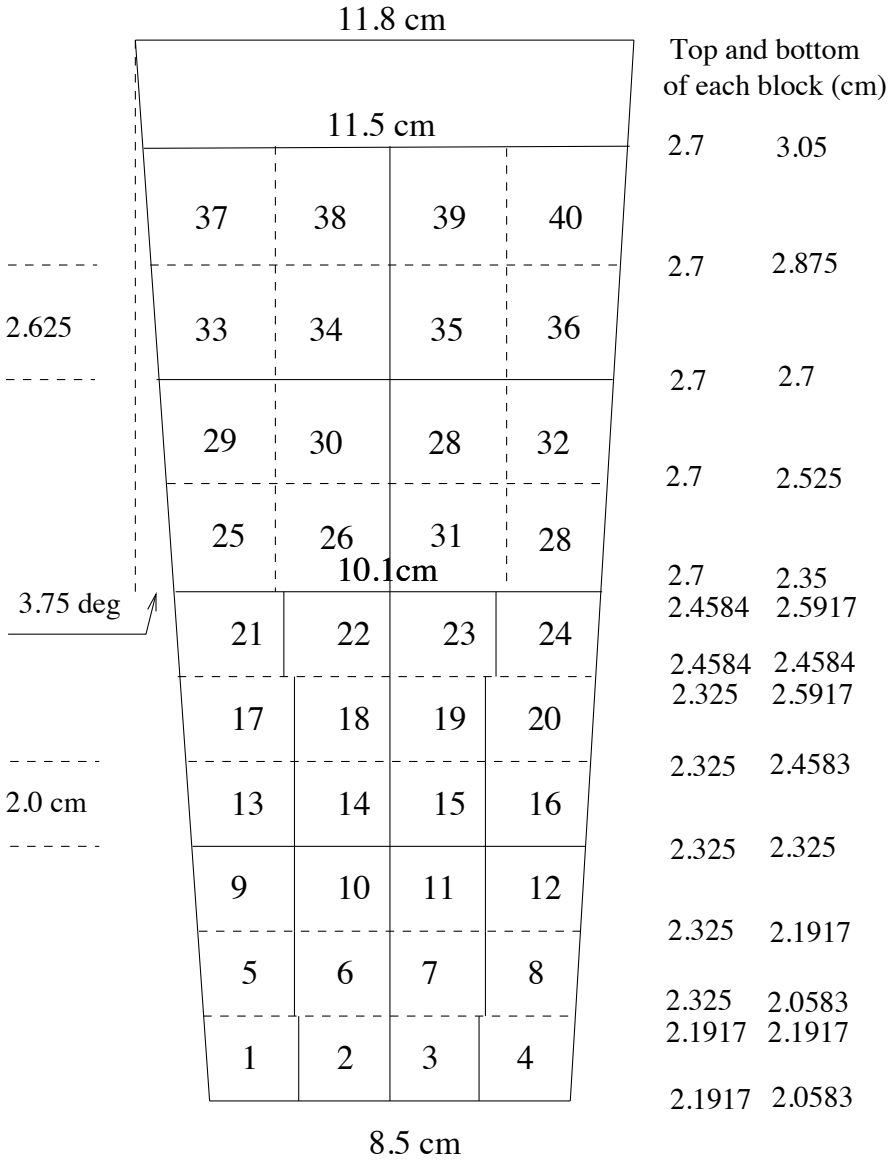


Figure 1: Proposed layout of the area on the BCAL face corresponding to the 40 SiPM sensors. The dimensions of the bases of each block are given for reference. This scheme results in a total of 9 different guides for the outer region and 11 different guides for the inner region, for a total of 20 different light guides (8 have a mirror image and 4 are rectangular). The vertical height of all outer guides is 2.625 cm and the vertical height of the inner guides is 2.0 cm. The proposed summing groups for SiPMs are enclosed by solid lines.

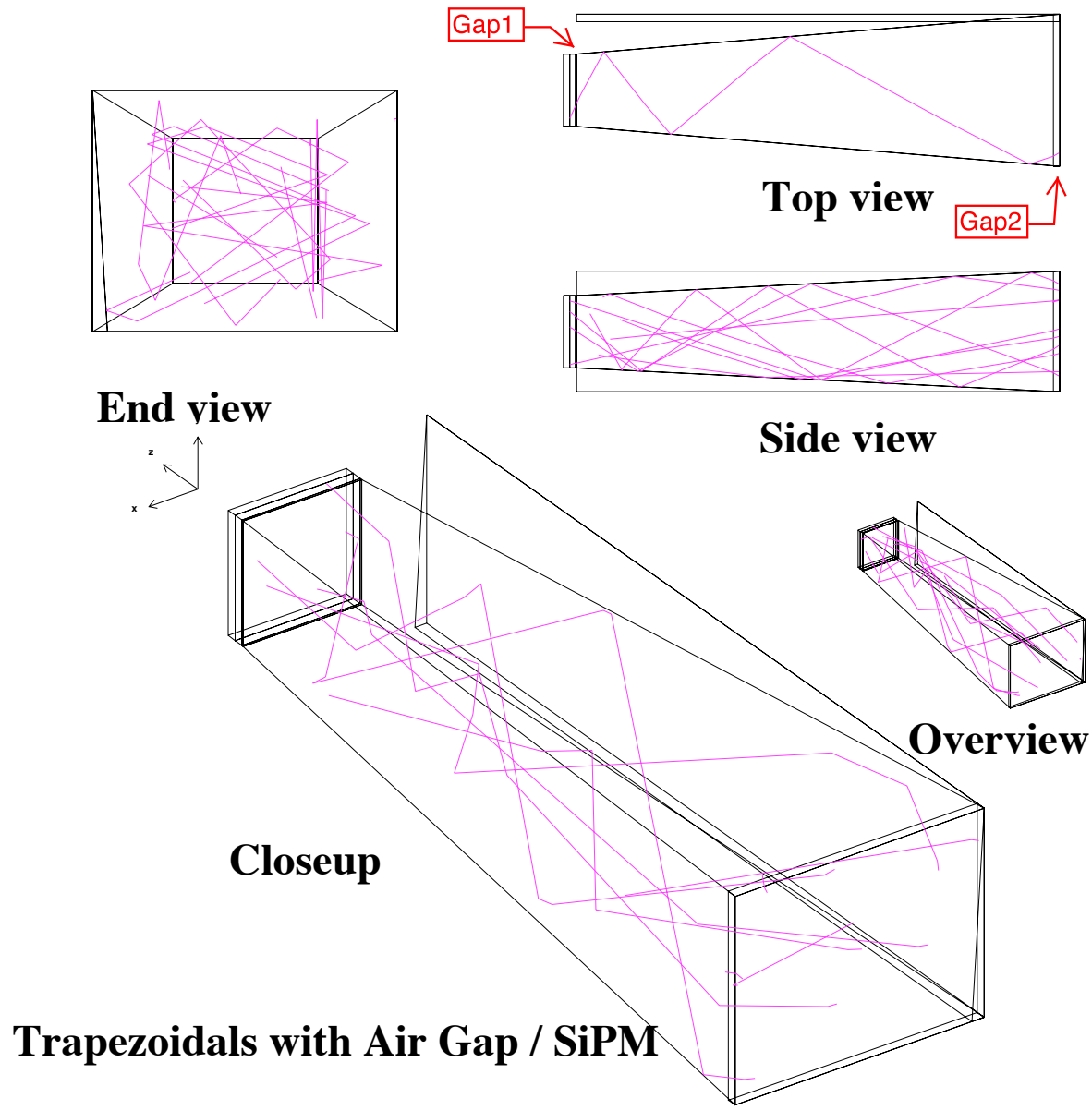


Figure 2: Geometry for light guide of SiPM #24 (inner top outside). The length of the light guide is 8 cm followed by a window and a sensitive volume representing the SiPM. The geometry allows for a gap preceding the light guide and following it. The widths of the gaps are adjustable and the material in the gap can be changed between air and lucite for comparative studies.

Table 3: Properties of core and cladding for SCSF-78MJ fibers.

| Layer | Material | Refractive Index | Density ($g/cm^3$) |
|---|---|---|---|
| Core | Polystyrene (PS) | 1.59 | 1.05 |
| Inner cladding | Polymethylmethacrylate (PMMA) | 1.49 | 1.19 |
| Outer cladding | Fluorinated polymer (FP) | 1.42 | 1.43 |

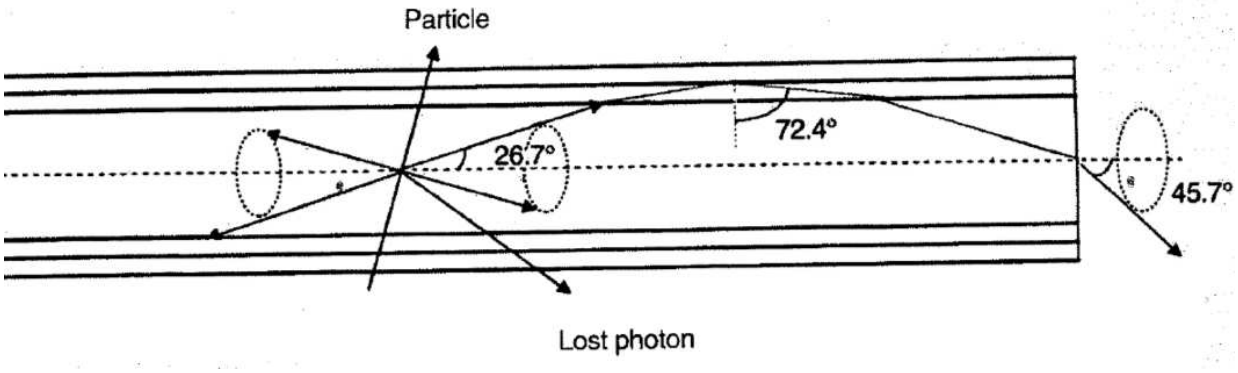


Figure 3: Sketch of trapped light rays inside Kuraray multiclad fibers, showing the maximum angles contained in the fibers. Reproduced from the Kuraray brochure on *Scintillation Materials*.

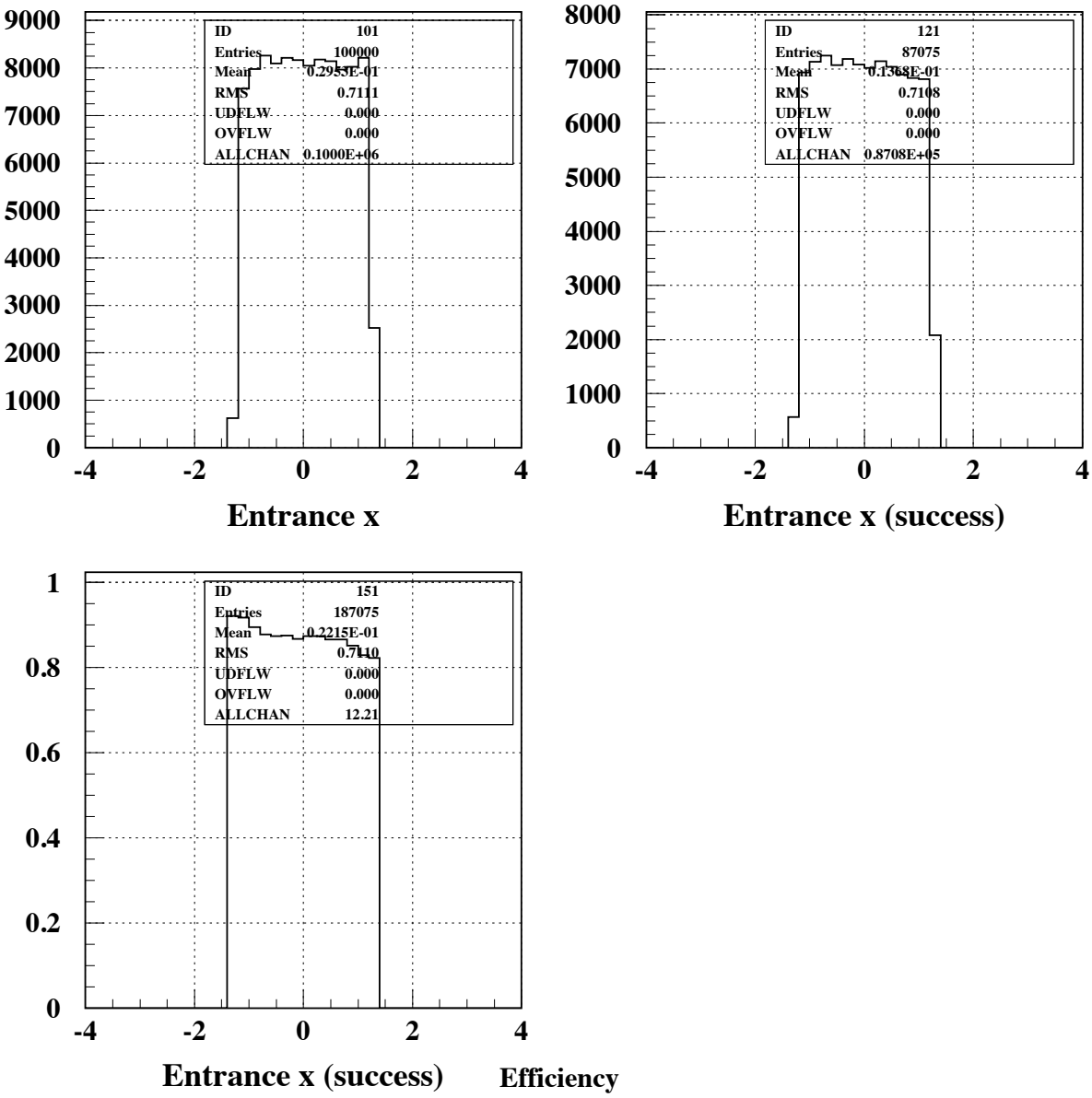


Figure 4: Length=8cm, 2mm lucite Gap1 between guide and SiPM. Top left) Input distributions as a function of the horizontal axis. Top right) Input distribution as a function of the horizontal axis for accepted photons. Bottom) Efficiency.

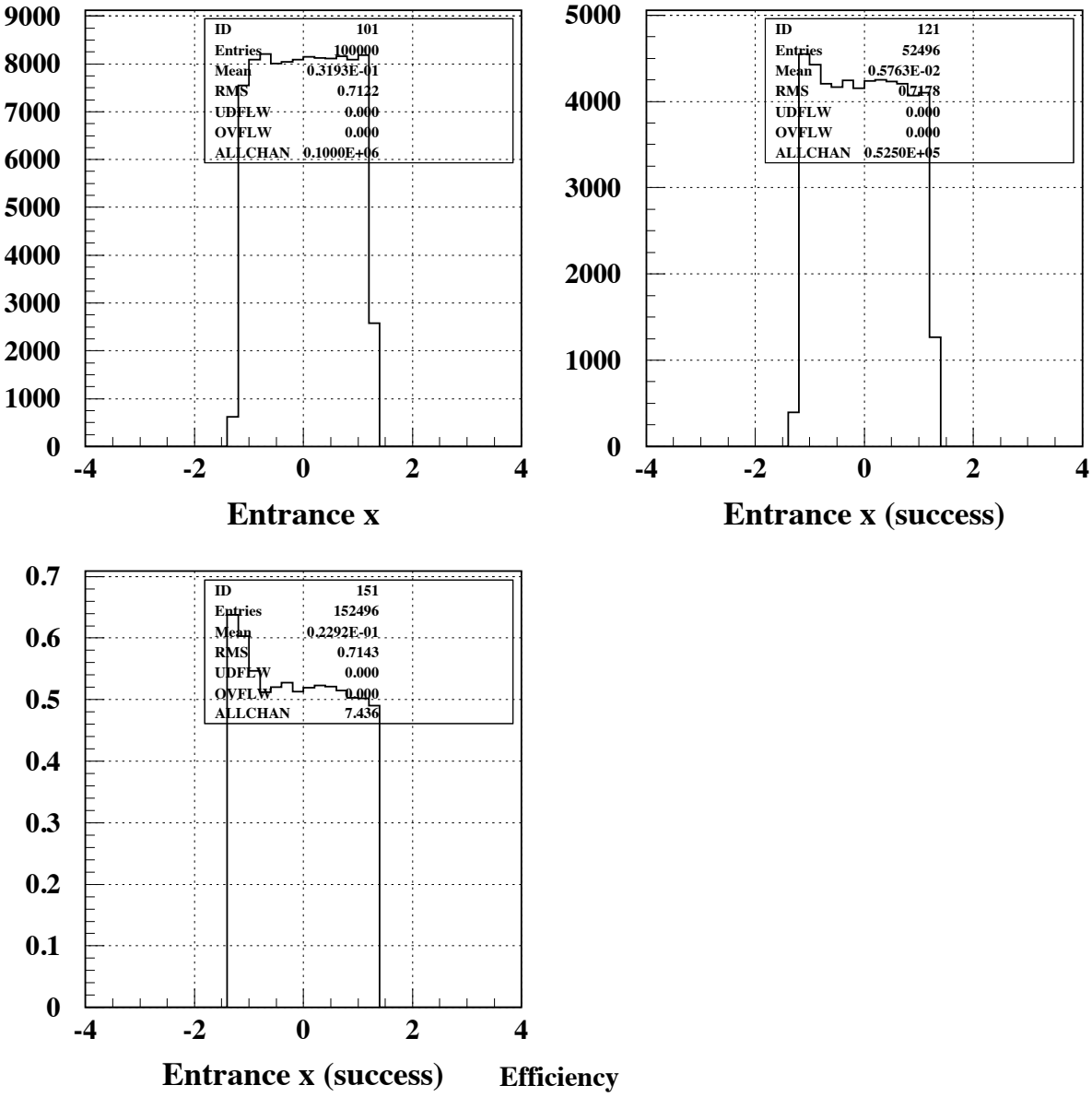


Figure 5: Length=8cm, 1mm air Gap1 between guide and SiPM. Top left) Input distributions as a function of the horizontal axis. Top right) Input distribution as a function of the horizontal axis for accepted photons. Bottom) Efficiency. The increased efficiency at low negative x is correlated with the 3.75° angle of the side of the light guide.

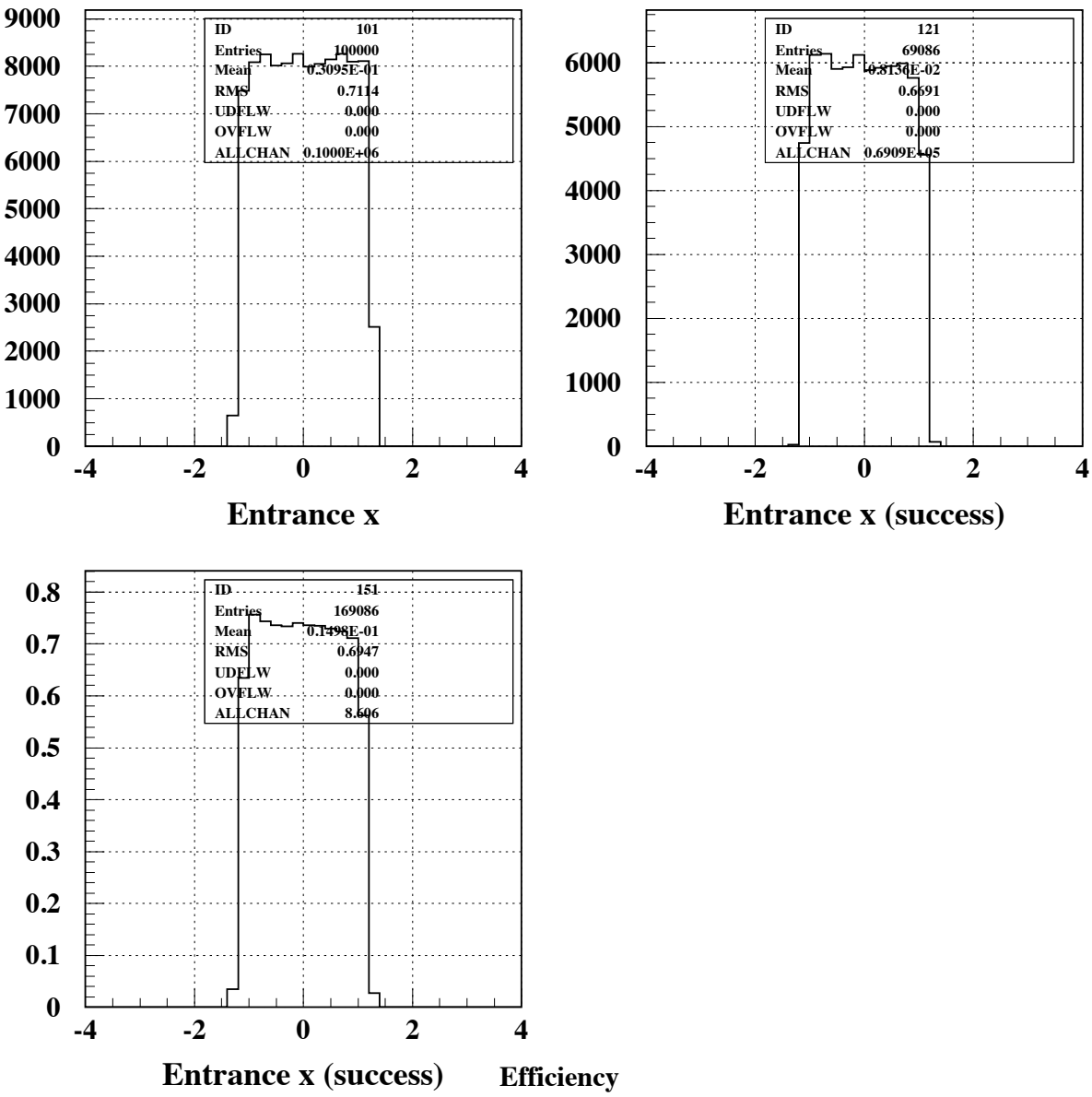


Figure 6: Length=8cm, 1mm air Gap2 between BCAL and guide. Top left) Input distributions as a function of the horizontal axis. Top right) Input distribution as a function of the horizontal axis for accepted photons. Bottom) Efficiency.

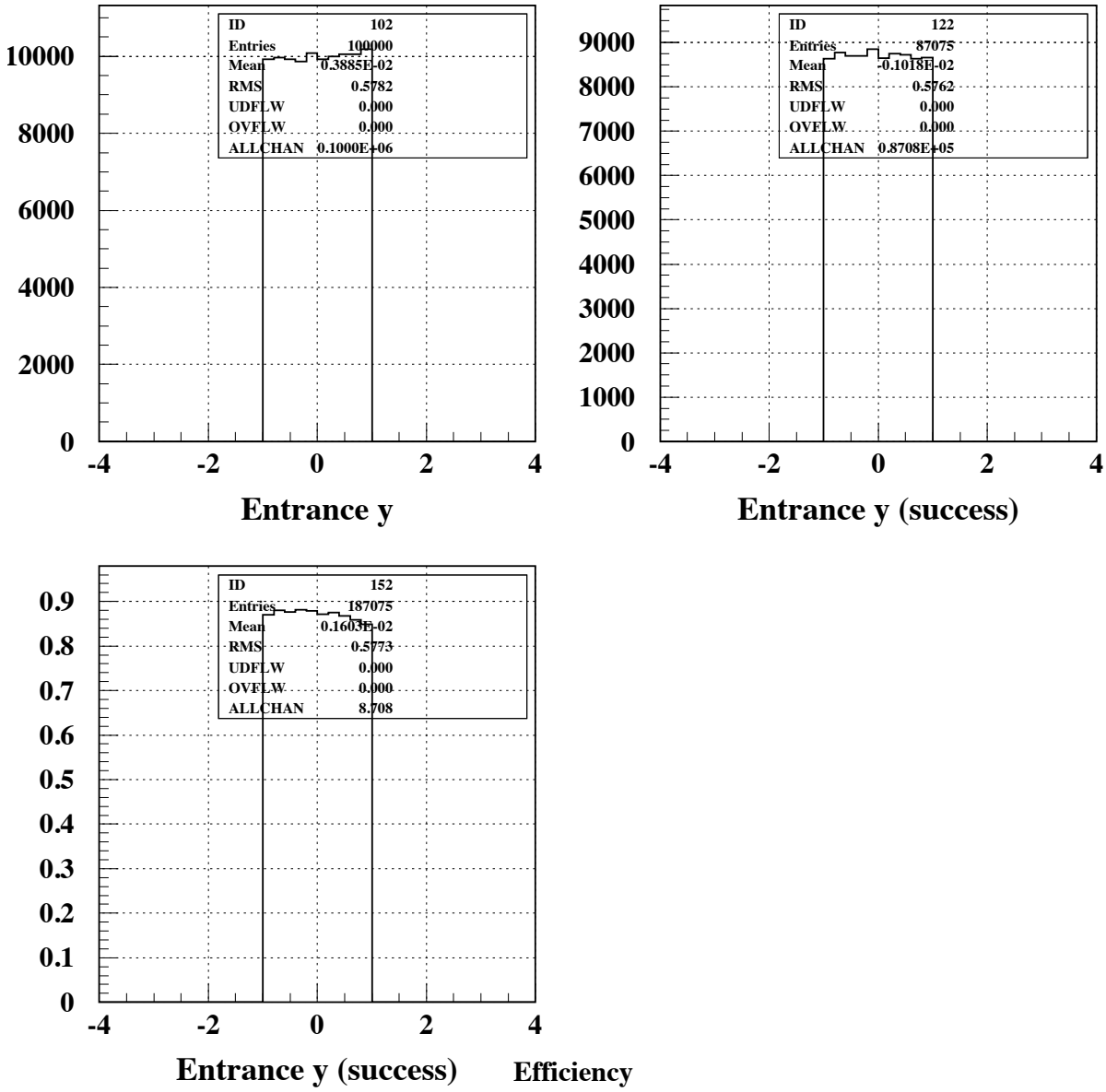


Figure 7: Length=8cm, 2mm lucite Gap1 between guide and SiPM. Top left) Input distributions as a function of the vertical axis. Top right) Input distribution as a function of the vertical axis for accepted photons. Bottom) Efficiency.

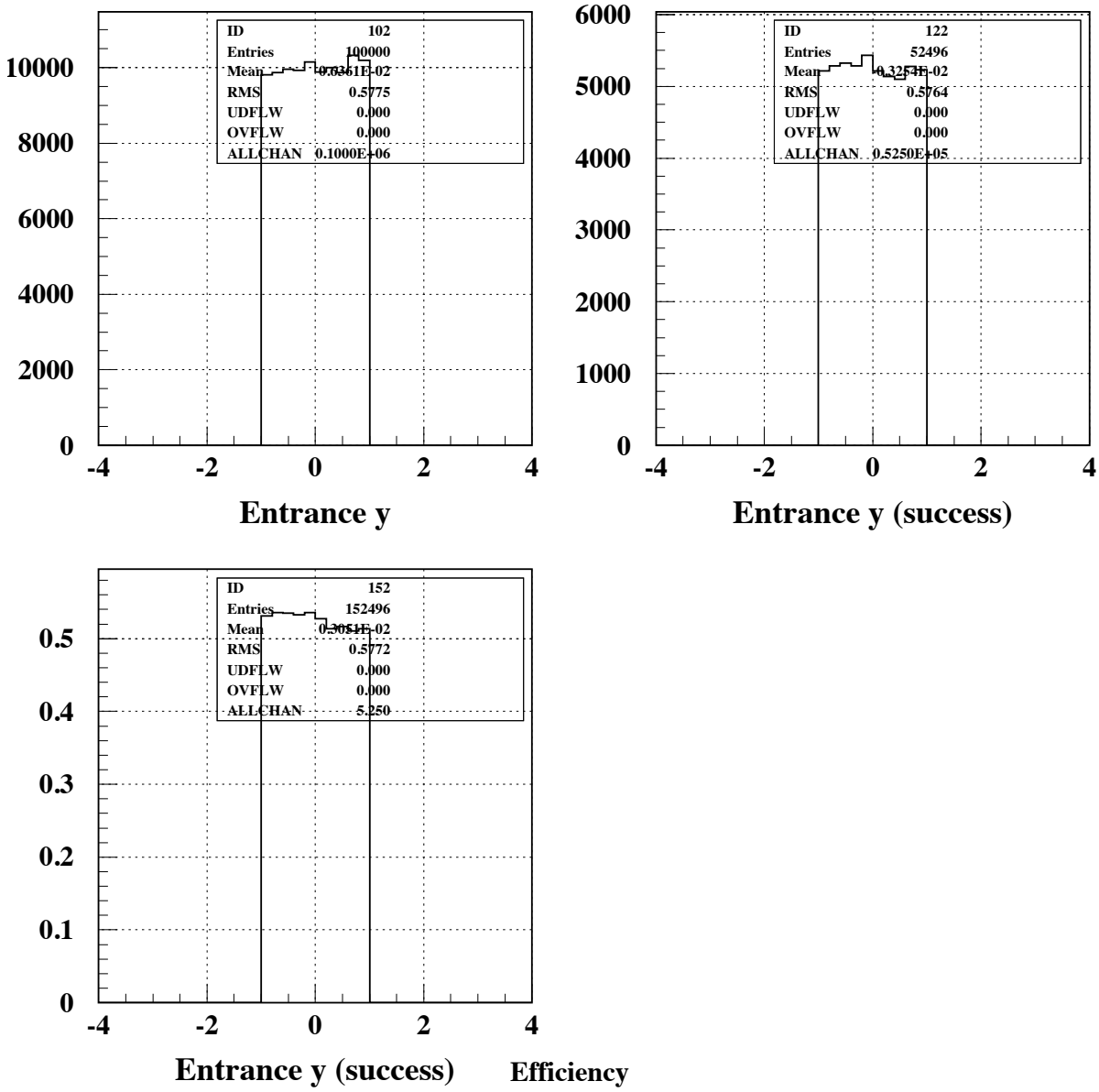


Figure 8: Length=8cm, 1mm air Gap1 between guide and SiPM. Top left) Input distributions as a function of the vertical axis. Top right) Input distribution as a function of the vertical axis for accepted photons. Bottom) Efficiency.

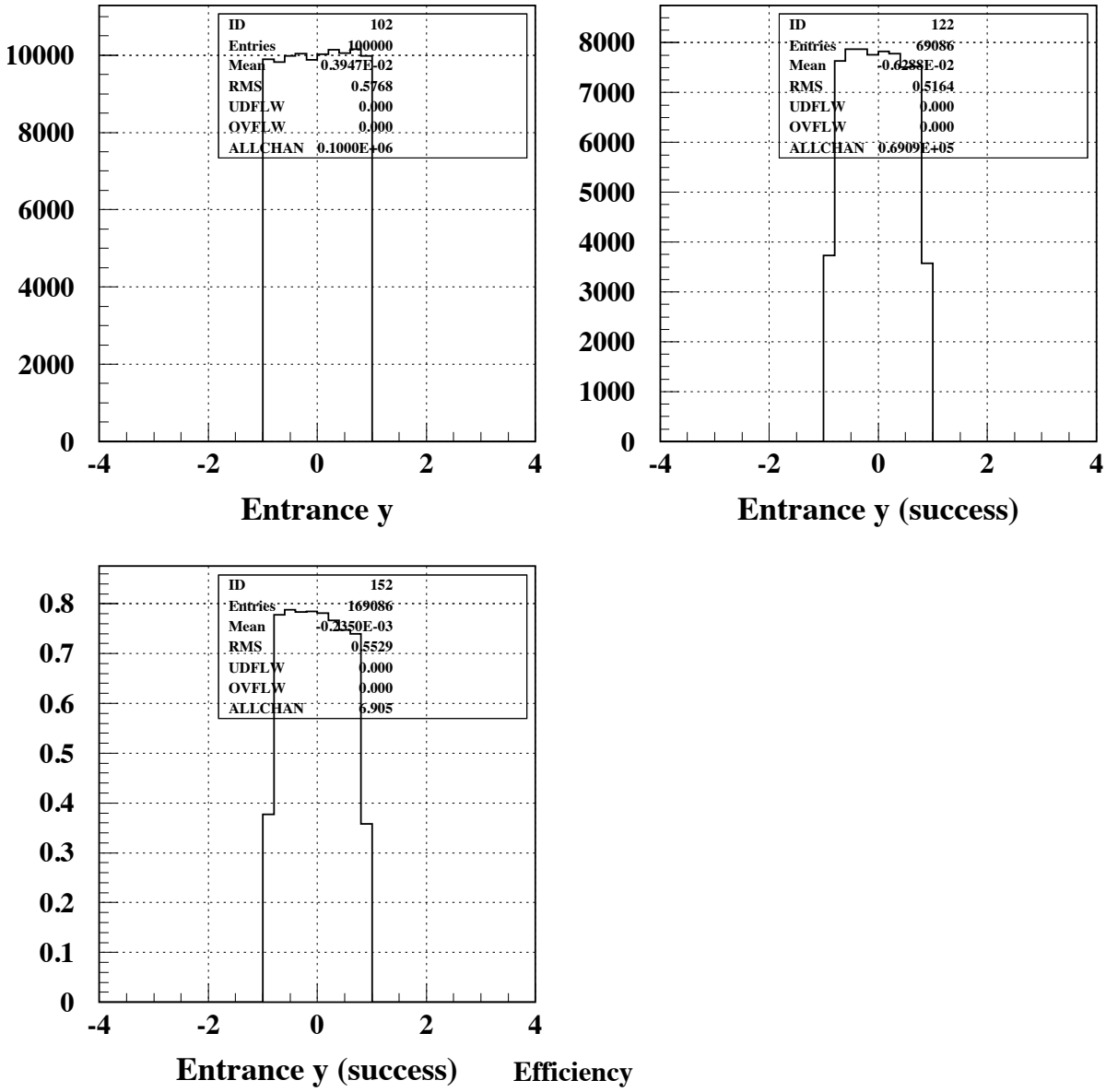


Figure 9: Length=8cm, 1mm air Gap2 between BCAL and guide. Top left) Input distributions as a function of the vertical axis. Top right) Input distribution as a function of the vertical axis for accepted photons. Bottom) Efficiency.

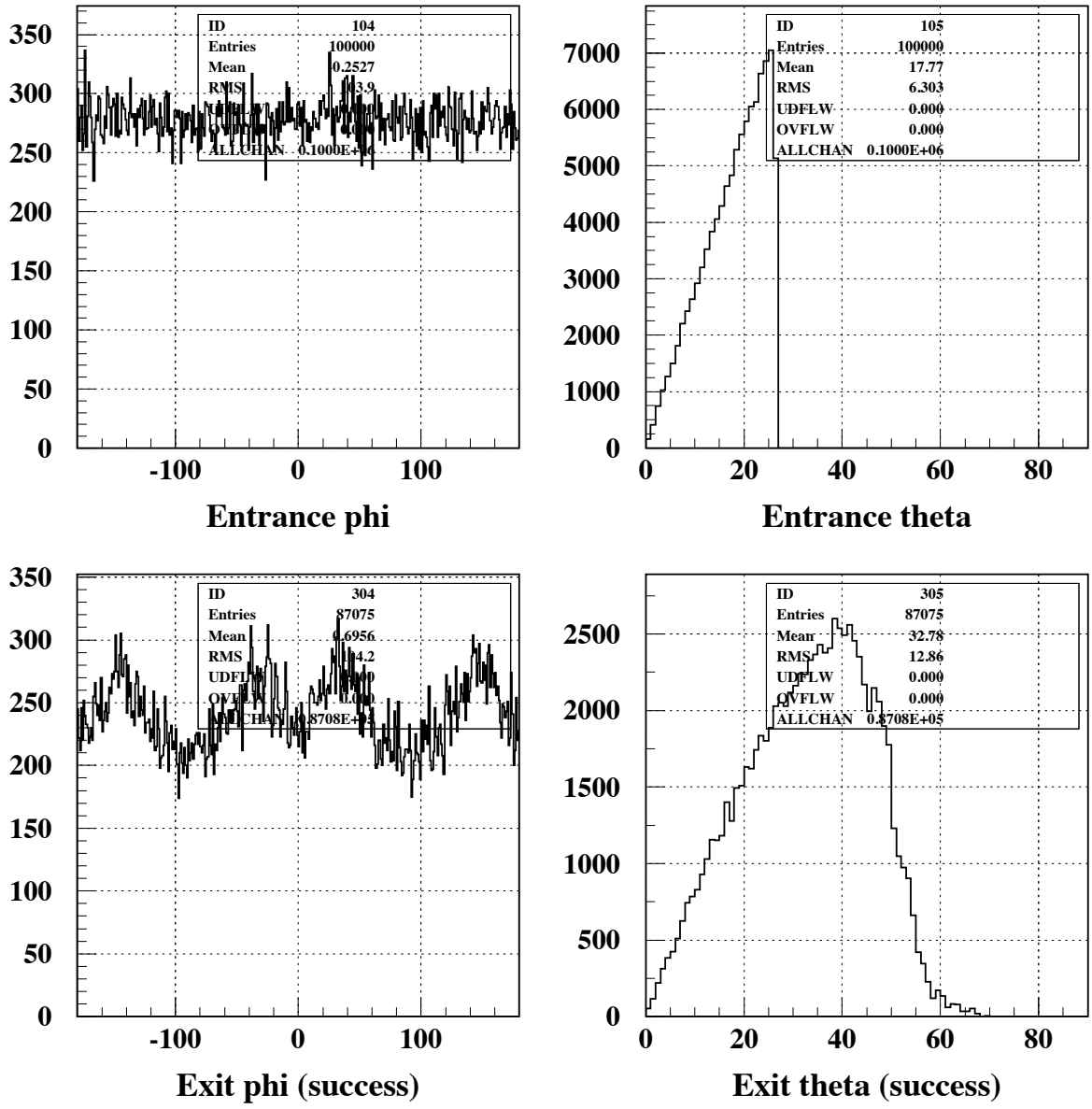


Figure 10: Length=8cm, 2mm lucite Gap1 between guide and SiPM. Top left) Distribution of input azimuthal angles. Top right) Distribution of input polar angles. Bottom left) Distribution of azimuthal angles at the exit. Bottom right) Distribution of polar angles at the exit.

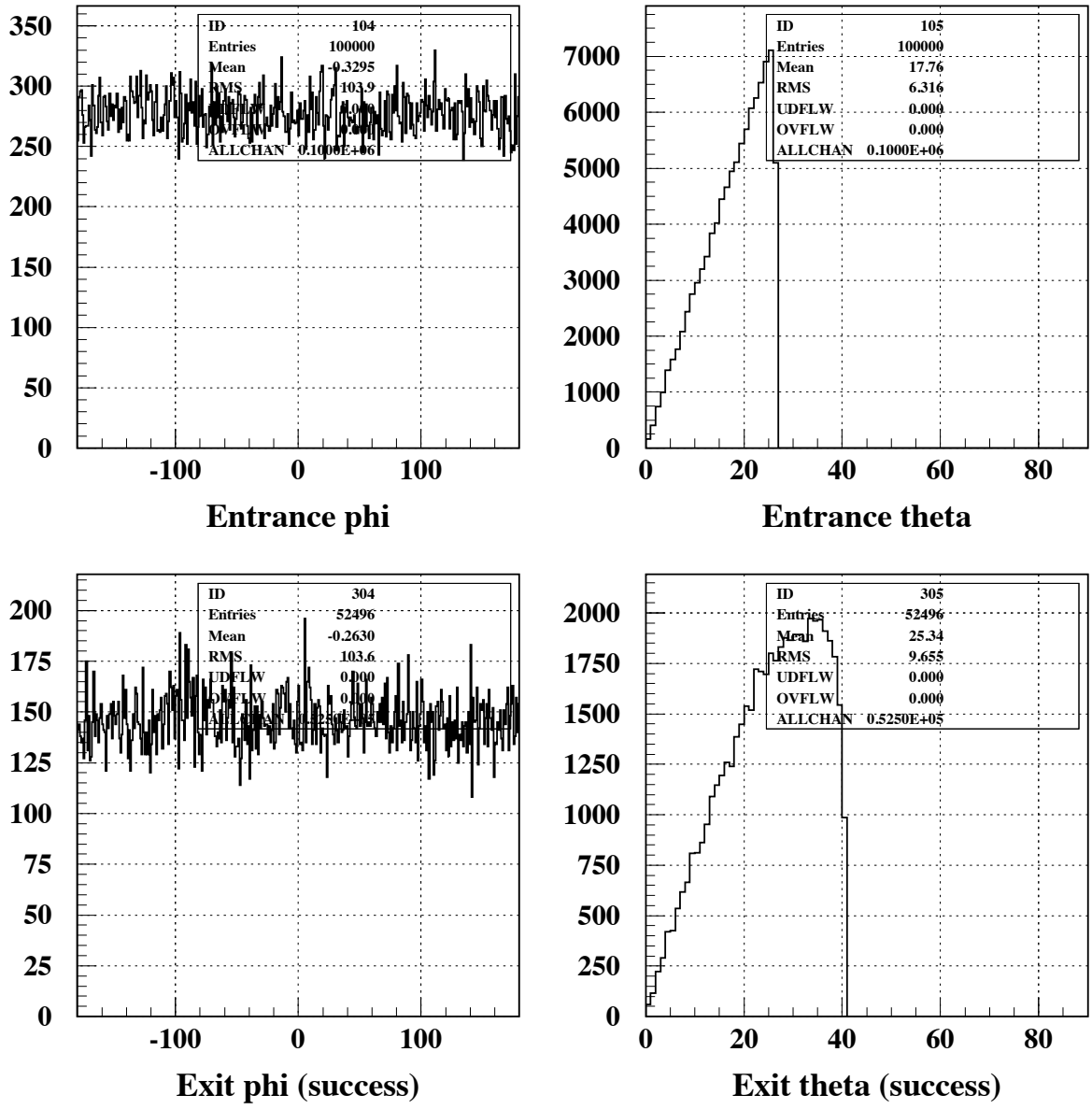


Figure 11: Length=8cm, 1mm air Gap1 between guide and SiPM. Top left) Distribution of input azimuthal angles. Top right) Distribution of input polar angles. Bottom left) Distribution of azimuthal angles at the exit. Bottom right) Distribution of polar angles at the exit.

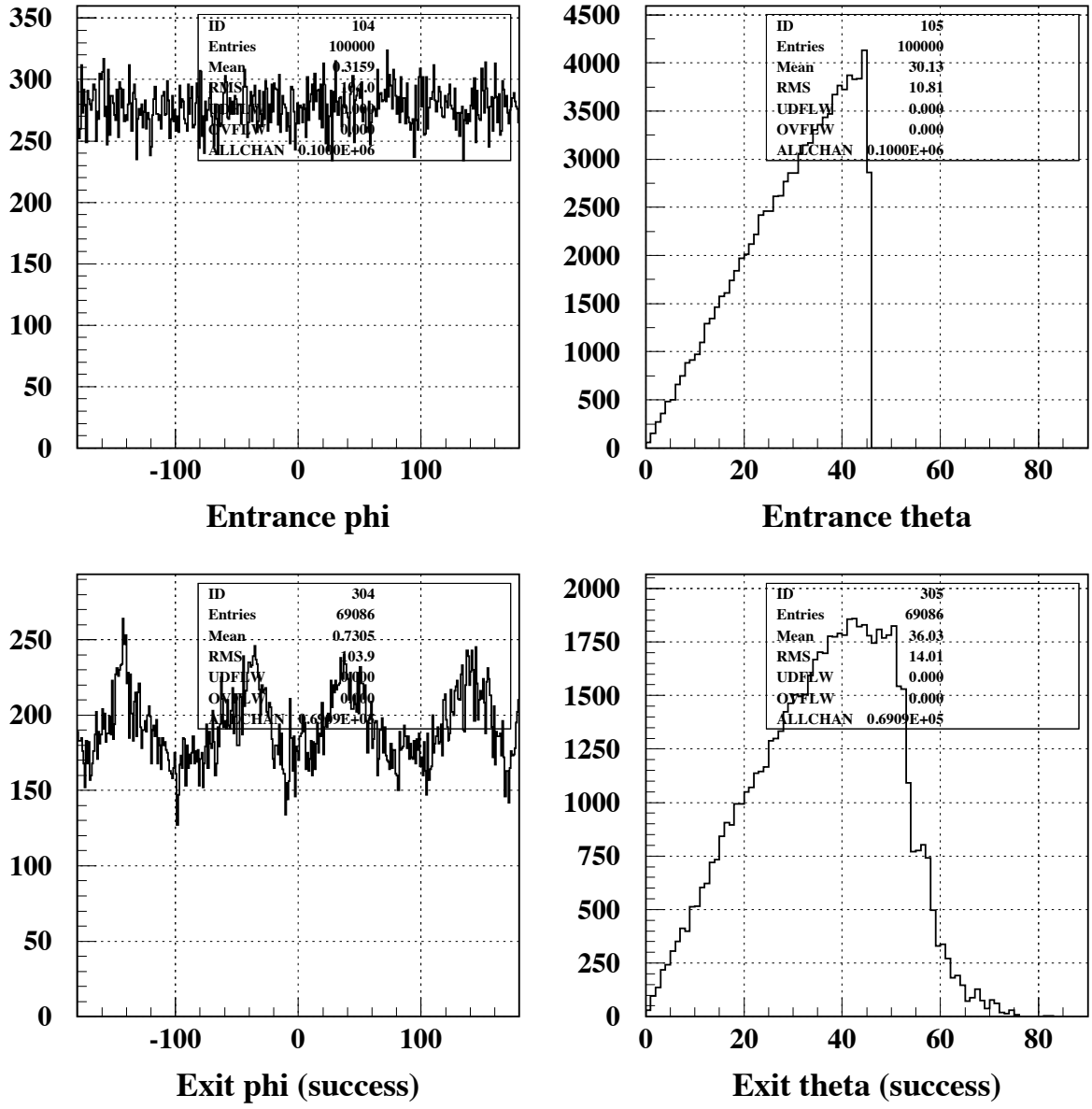


Figure 12: Length=8cm, 1mm air Gap2 between BCAL and guide. Top left) Distribution of input azimuthal angles. Top right) Distribution of input polar angles. Bottom left) Distribution of azimuthal angles at the exit. Bottom right) Distribution of polar angles at the exit.

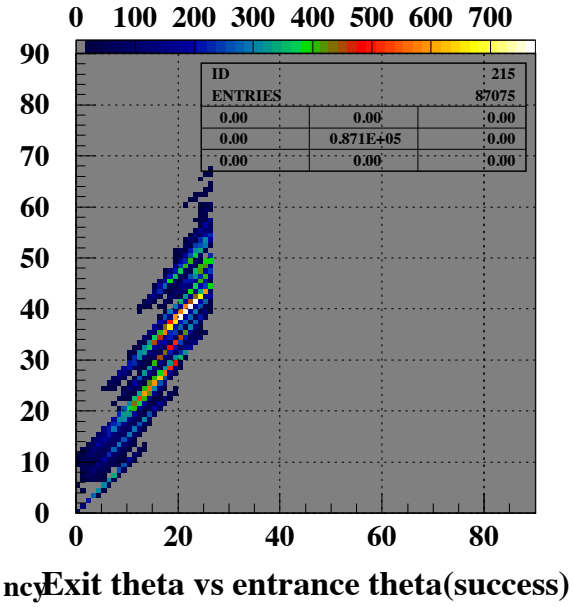


Figure 13: Length=8cm, 2mm lucite Gap1 between guide and SiPM. Exit polar angle vs input polar angle for accepted photons.

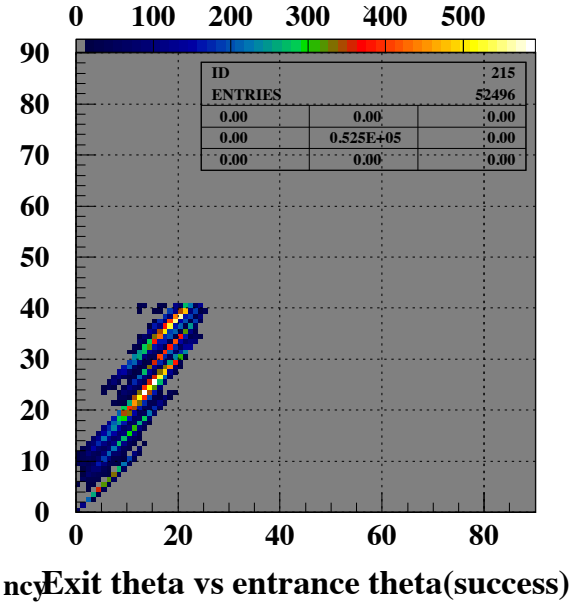


Figure 14: Length=8cm, 1mm air Gap1 between guide and SiPM. Exit polar angle vs input polar angle for accepted photons.

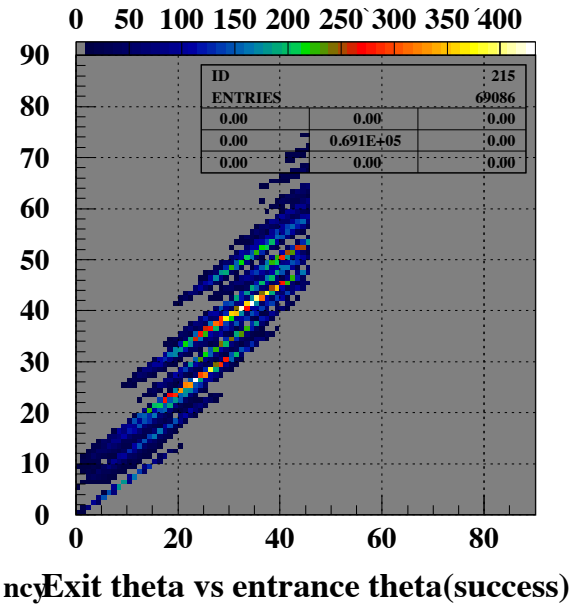


Figure 15: Length=8cm, 1mm air Gap2 between BCAL and guide. Exit polar angle vs input polar angle for accepted photons.

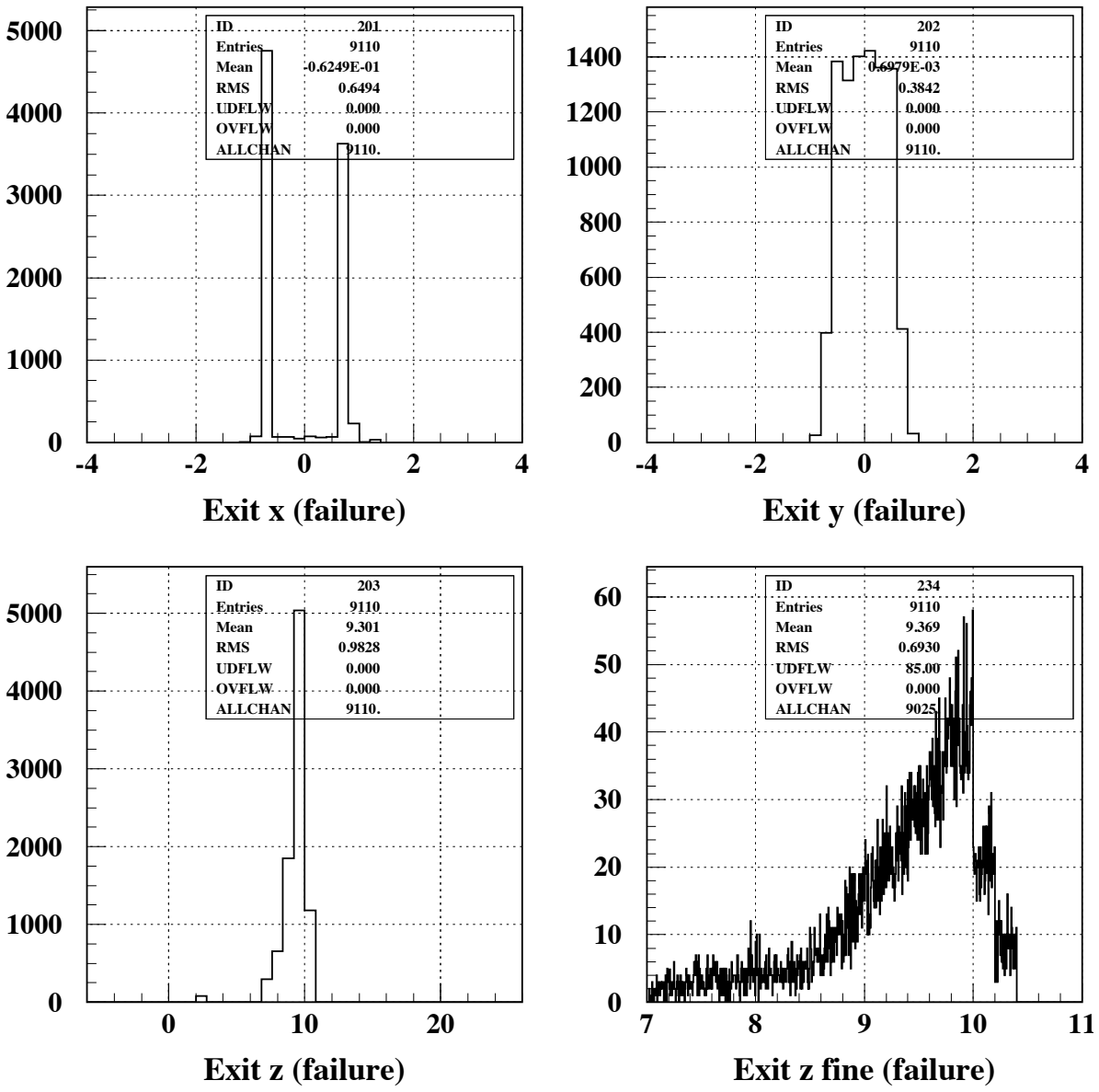


Figure 16: Length=8cm, 2mm lucite Gap1 between guide and SiPM. Distribution of exit locations in x, y and z (and z on a fine scale) for photons which failed to reach the sensitive volume.

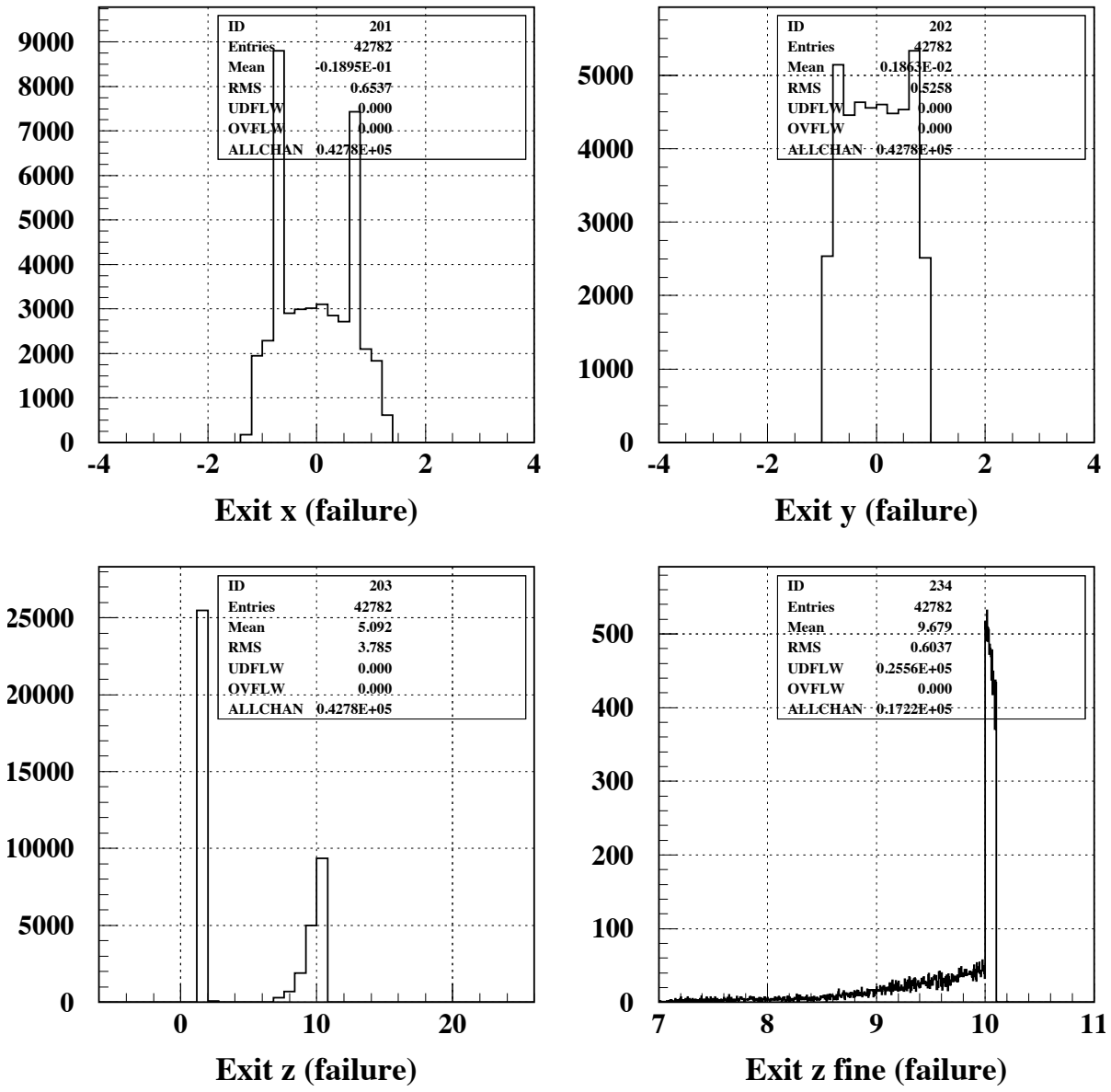


Figure 17: Length=8cm, 1mm air Gap1 between guide and SiPM. Distribution of exit locations in x, y and z (and z on a fine scale) for photons which failed to reach the sensitive volume.

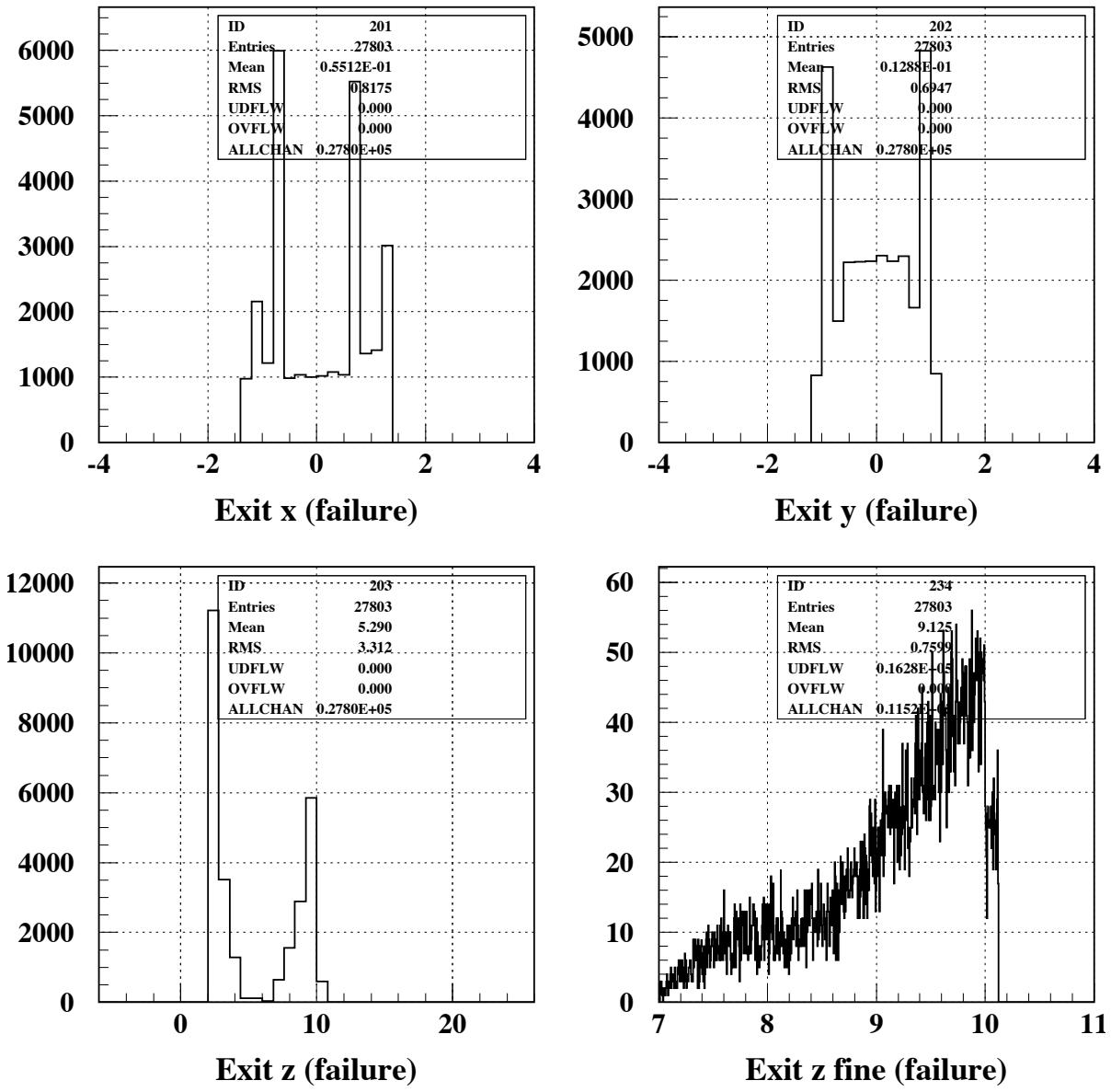


Figure 18: Length=8cm, 1mm air Gap2 between BCAL and guide. Distribution of exit locations in x, y and z (and z on a fine scale) for photons which failed to reach the sensitive volume.

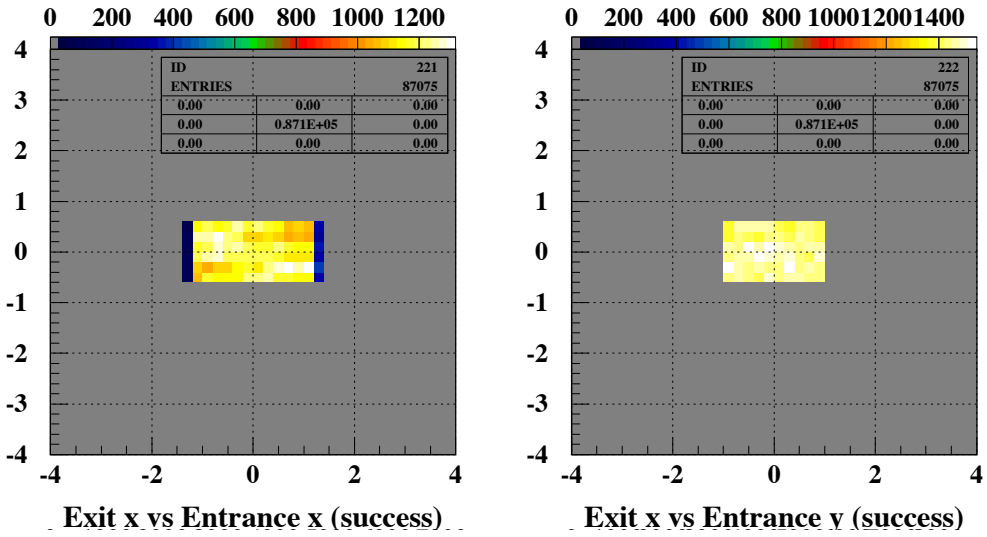


Figure 19: Length=8cm, 2mm lucite Gap1 between guide and SiPM. Correlation between exit and input positions for photons that reach the sensitive volume. The distributions show that the light is very well mixed and the correlations between input and output positions are weak.

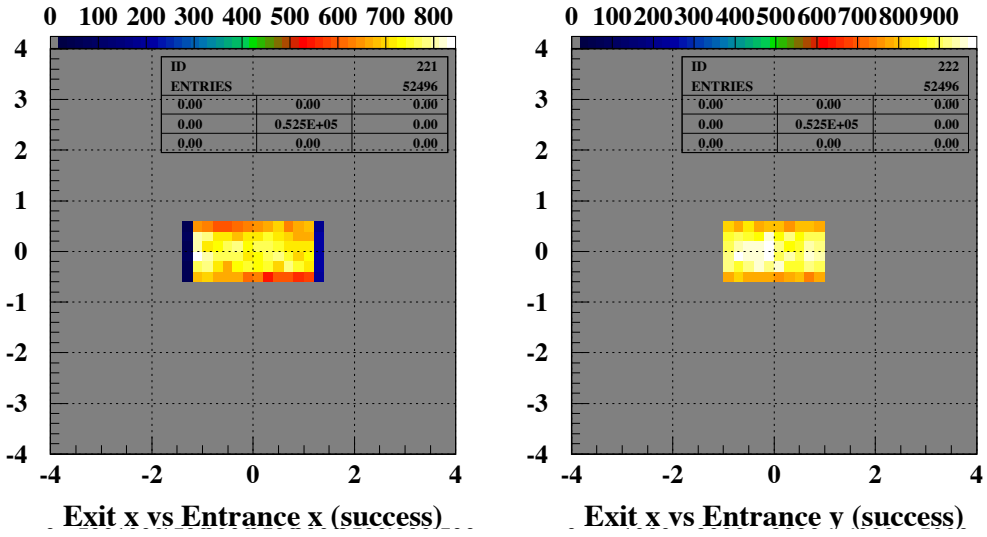


Figure 20: Length=8cm, 1mm air Gap1 between guide and SiPM. Correlation between exit and input positions for photons that reach the sensitive volume. The distributions show that the light is very well mixed and the correlations between input and output positions are weak.

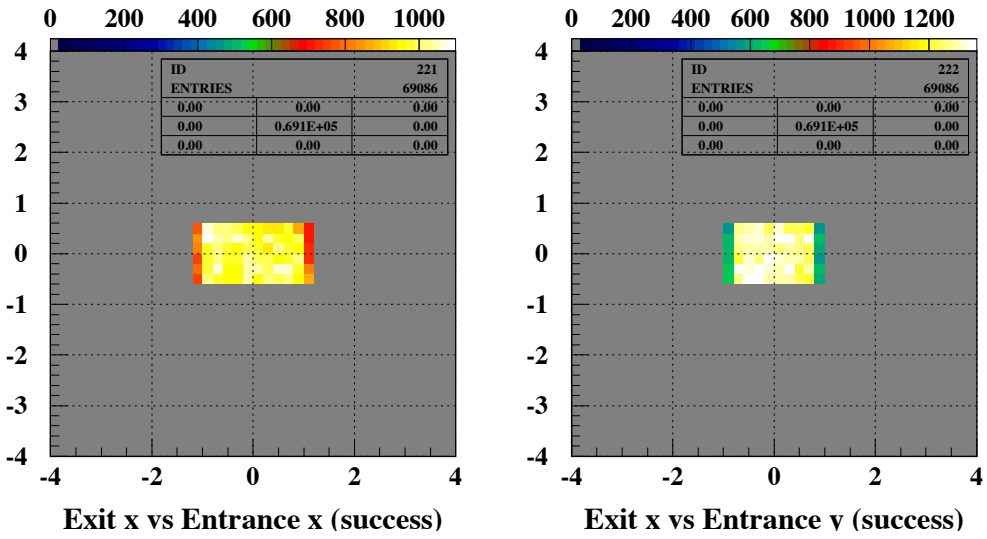


Figure 21: Length=8cm, 1mm air Gap2 between BCAL and guide. Correlation between exit and input positions for photons that reach the sensitive volume. The distributions show that the light is very well mixed and the correlations between input and output positions are weak.

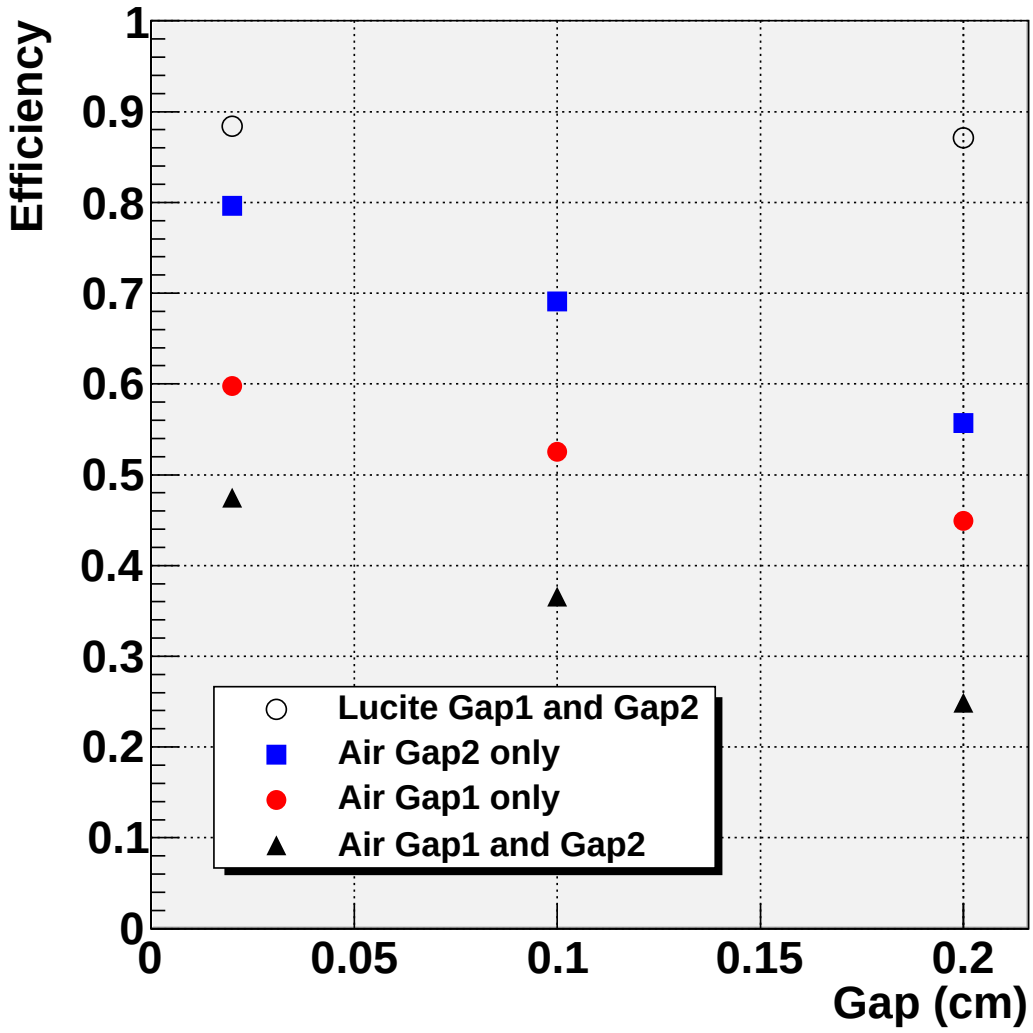


Figure 22: Light collection efficiency as a function of the various gap widths. Gap1 is the gap between the light guide and the SiPM, and Gap2 is located between the calorimeter module and the light guide. For reference, the efficiency is calculated for an exit Gap 1 with lucite and no gap at the entrance (plotted as open circles). There is a finite collection efficiency at zero gap width, and the efficiency decreases linearly as the gap increases. However, the dependence on the gap size is more pronounced for air gaps than it is for a lucite gap.